CHAPTER VII

CHARACTERIZATION OF CHOPPED GLASS FIBER REINFORCED POLYBENZOXAZINE FOAM COMPOSITE

7.1 Abstract

Because of the limited understanding of the behaviors of fiber reinforced polybenzoxazine foam due to the shortage of involving researches, this work presents the influence of glass reinforcing fiber on mechanical, physical, and thermo mechanical properties of polybenzoxazine foam composite. The study shows that the compressive modulus and strength increased by 75.2% and 52.5%, respectively, when the amount of reinforcing fiber was 5 wt%. Dynamic mechanical analysis (DMA) indicated that the Tg of the foam composite was systematically increased from 184 °C of the neat foam to 190 °C of 5wt% glass fiber reinforced foam composite. Furthermore, the rubbery plateau modulus also increased as the fiber content. However, when the amount of the fiber was higher than 3 wt%, inevitable massive void due to mechanical mixing was appeared in the resulting foam.

(Key-words: Benzoxazine; Benzoxazine foam; Glass fiber reinforced)

7.2 Introduction

Phenolic foams generally exhibit excellent fire properties, such as low flammability, low peak heat release rate (PHRR), no dripping during combustion, and low smoke density [1-4]. However, the traditional phenolic resins still suffer from some disadvantages, such as release of any by-products during the curing reactions, need of strong acid catalysts, toxic raw materials, formation of voids, and limited shelf life [2, 5]. On the other hand, polybenzoxazine can be able to not only overcome these shortcomings, but also presents many characteristics not found in traditional phenolic resins, such as high thermal stability, excellent mechanical properties, easy processibility, low water absorption, near zero shrinkage after polymerization, and molecular design flexibility [6, 7]. Thus, polybenzoxazine becomes an excellent candidate resin to replace traditional reactants for the foam manufacturing. Generally, to achieve higher mechanical performance and thermal stability of foam materials, they are frequently manufactured in the form of fiber reinforced composite. Among many types of reinforcing fibers usually used in phenolic foams, glass fiber is one of the most favorites [3, 5, 8]. Since there are very few researches involving in polybenzoxazine foam, the understanding of the behavior of the fiber reinforced polybenzoxazine foam is limited. Therefore, study of the influence of glass reinforced fiber on polybenzoxazine foam is absolutely attractive. According to our previous research [2], it was found that the resulting polybenzoxazine foam using azodicarbonamide (AZD) as a blowing agent demonstrated a uniform foamed structure, and at about 3 wt% AZD it provided a good balance between mechanical properties and weight of the polybenzoxazine foam. In this work, investigation on the influence of reinforcing fiber on the manufacturing, physical, and mechanical properties of the foam was performed. Optimum fiber content, demonstrating the most appropriate equality between properties of the foam and controllability of the foaming process, is also reported and discussed.

7.3. Experimental

7.3.1 Materials

The benzoxazine resin used in this research is based on bisphenol-A, aniline, and formaldehyde. Bisphenol-A (97%) and para-formaldehyde (95%) were purchased from Sigma-Aldrich Company. Aniline (99%) was purchased from Panreac Quimica SA Company, and azodicarbonamide (AZD, Supercell-VR207) used as a blowing agent was provided by A. F. Supercell Co., Ltd. Untreated chopped glass fiber (Jushi group Ltd.) with average length of 3 mm was selected for reinforcement.

7.3.2 Foam Composite Preparation

The benzoxazine monomer synthesis is followed our previous work [2]. The benzoxazine monomer was grounded into fine powder and mixed with 3 wt% AZD before adding glass fiber with different weight ratios, i.e. 1, 3, and 5 wt%. The mixture was melt-mixed at about 110 °C until a homogeneous mixture was obtained; followed by transferring into an aluminum mold and heating from 30° to 210 °C using a heating rat of 1 °C/min.

7.3.3 Characterization of Foam Composite

The densities of the foam samples were determined by weighing the geometrically shaped foam and dividing the weight by measured volume. The microstructures of the foams were observed on JEOL-JS 5800LV scanning electron microscopy (SEM) and Olympus SZ-4045-TR optical microscope. An INSTRO universal testing instrument (Model 4502) with a 150 kN static load cell was used to determine uniaxial compression properties of the resulting foams. Cylindrical foams specimens were compressed with a crosshead speed of 2.5 mm/min. Compressive modulus were calculated at the steepest slope of the stress–strain curve, and compressive strength was determined at the fracture failure of the specimen. DMA (NETZSCH DMA 242) was used to characterize the thermomechanical properties of the foams. The thermograms were obtained with a heating rate of 5 °C/min. Storage modulus (E') and loss tangent (tan δ) were reported in the thermograms. The glass

transition temperature of the foams was determined at the maximum point of loss tangent curve.

7.4. Results and Discussion

The theoretical and measured densities of the resulting foams at various fiber contents are summarized in Table 7.1. It is clear that the foam density increases with fiber content, and the measured values are higher than the theoretical ones, except at 5wt% fiber content. It implies that the reinforcing fiber inhibited foam expansion in the foaming process. However, at the high fiber content, the negative deviation from the theoretical value was caused by the presence of unavoidable defect due to the high viscosity of fiber melt-mixed precursor, which was created during the mechanical mixing process. Furthermore, this result strongly agrees with the morphology of the foams which will be discussed further. This outcome also corresponds to the other types of fiber reinforced foam composites [9, 10]. The cellular structures of the resulting foams were obtained by using 3 times magnification of an optical microscope. Figure 7.1a demonstrates the morphologies of the cell structures affected by the presence of the short fiber with different fiber contents. From the examination, the neat polybenzoxazine foam revealed uniform foam structure with an orange color, but fiber reinforced polybenzoxazine foams showed denser porous structure combined with massive voids. In addition, it could be found that the denseness and large void content tended to increase as more fiber was added, which conforms to their densities.

SEM was used to examine the distribution and bonding aspects of reinforcing fiber in the foam matrix. Figure 7.1b reveals a razor cut surface of 3wt% of fiber reinforced foam. As seen in the figure, the reinforcing fibers are randomly distributed and appear embedded only in the cell walls, and there is no fiber penetrating through the foam cells. The enlargement shown within the figure reveals that the reinforcing fiber is not surrounded with the air gaps, which represents very good wetting and adhesion between glass fiber and polybenzoxazine matrix even when fiber surface treatment was not used in this study. This result also illustrates good matching between the glass fiber and polybenzoxazine matrix.

Figure 7.2 shows the compressive strength and modulus of the foams as a function of fiber content. As observed in the figure, both average value of foam strength and modulus continually increase as a function of fiber content. In addition, with small amount of reinforcing fiber (up to 3wt%. fiber content), the compressive modulus and strength of the foams were increased rapidly by 53.8% and 45.6%, respectively. The sharp increase of the strength and modulus is due to the fiber reinforcing effect which leads to the enhancement of the compressive properties of the resulting foams. This phenomenon is a good agreement with the rule of mixture, which the properties of the resulting foam composites depend on the volume fraction of polymer matrix and reinforcing fiber. Moreover, there are other reasons proposed for strength improving of foam composites, i.e. formation of multiple crack site and/or multiple crack branching, better adhesion between reinforcing fiber and matrix, which are able to delay the fracture processes of foam composites [11, 12]. However, at the higher fiber content, the modulus and strength were increased more slowly with increased fiber content. Especially, due to the insignificantly change of the strength, optimal fiber content is found at around 3wt%. This result complies with the morphology of the resulting foams, which structural defect plays an important role in the deterioration of the compressive properties at the high fiber content. This behavior is also noticed in other related works [5, 10].

Figure 7.3a shows the effect of the fiber content on the storage modulus (E') of the foam composites with different glass fiber contents. In order to achieve reliable DMA data, the selected specimens without structural defect were employed in this test to avoid uncertainty of the thermomechanical response. As a similar trend with the observation for compressive modulus, the glassy stage plateau modulus of the resulting foams systematically increased with the glass fiber content. Furthermore, the rubbery plateau modulus of the foams was also systematically increased, which reveals the sturdiness of the foams after their glass transition stage. As discussed by M. Abdalla *et al.*, the increase in the rubbery plateau modulus is due to the difference between the modulus of reinforcing fiber and the rubbery resin and the limitation of polymer mobility caused by polymer and reinforcing fiber interaction [13]. Figure 7.3b shows tan δ versus temperature curve of the foam composites at various fiber contents. Although, the falling of the storage modulus

does not show a distinct increasing trend, the glass transition temperature observed based on the relaxation peak of tan δ increases considerably with the fiber content from 184° to190 °C of plain and 5 wt% fiber content respectively, as summarized in Table 7.1. The increment of the glass transition temperature and rubbery plateau modulus of foam composites was due to the fiber reinforcing effect analogous to other related works [13-15].

7.5 Conclusions

A new type of glass fiber reinforced phenolic foam composite was successfully prepared with our noncomplex and economical foaming method. The SEM micrograph shows a random distribution of the fiber in the foam matrix, and very good adhesion between the fiber and the matrix can be observed. From the DMA thermogram, the glass transition temperature of the foam composites shows an improvement of 6 °C at 5 wt% fiber loading compared with the neat one. Approximately 3wt% of fiber content is the most appropriate content, providing a good balance between the mechanical properties of the foams and controllability of the foaming process.

7.6 Acknowledgements

This research was financially supported by the Thailand Research Fund (TRF), the Postgraduate Education and Research Program in Petroleum and Petrochemical Technology (ADB) Fund (Thailand), and the Ratchadapisake Sompote Fund, Chulalongkorn University.

7.7 References

1. Rodrigue-Perez, M.A. (2005) Crosslinked polyolefin foams: production, structure, properties, and applications. Advances in Polymer Science, 184, 97-126.

2. Lorjai, P., Wongkasemjit, S., and Chaisuwan, T. (2009) Preparation of polybenzoxazine foam and its transformation to carbon foam. Materials Science and Engineering: A, 527, 77-84.

3. Shen, H. and Nutt, S. (2003) Mechanical characterization of short fiber reinforced phenolic foam. Composites Part A, 34, 899-906.

4. Tseng, C.J. and Kuo, K.T. (2002) Radiative thermal properties of phenolic foam insulation. Journal of Quantitative Spectroscopy & Radiative Transfer, 72, 349-359.

5. Kumar, K.S.S., Nair, C.P.R., and Ninan, K.N. (2008) Silica fiber–polybenzoxazine–syntactic foams; processing and properties. Journal of Applied Polymer Science, 107,1091-1099.

6. Ning, X. and Ishida, H. (1994) Phenolic materials via ring-opening polymerization: Synthesis and characterization of bisphenol-A based benzoxazines and their polymers. Journal of Polymer Science - Polymer Chemistry Edition, 32, 112-119.

7. Kumar, K.S.S., Nair, C.P.R., and Ninan, K.N. (2008) Mechanical properties of polybenzoxazine syntactic foams. Journal of Applied Polymer Science, 108, 1021-1028.

8. Shen, H., Lavoie, A.J., Nutt, S.R. (2003).Enhanced peel resistance of fiber reinforced phenolic foams. Composites Part A, 34, 941-948.

9. Karthikeyan, C.S., Sankaran, S., and Kishore (2004) Elastic behavior of plain and fibre-reinforced syntactic foams under compression. Materials Letters, 58 995-999.

10. Karthikeyan, C.S., Murth, C.R.L., Sankaran, S., and Kishore (1999) Characterization of reinforced syntactic foams using ultrasonic imaging technique. Bulletin of Materials Science, 22, 811-815.

11. Vaikhanksi, L. and Nutt, S.R. (2003) Synthesis of composite foam from thermoplastic microsphere sand 3D long fibers. Composites Part A, 34, 755-763.

12. Saha, M.C., Kabir, M.E., and Jeelani, S. (2008) Enhancement in thermal and mechanical properties of polyurethane foam infused with nano particles Materials Science & Engineering, A, 479, 213-222.

13. Abdalla, M., Dean, D., Adibempe, D., Nyairo, E., Robinson, P., and Thompson, G. (2007) The effect of interfacial chemistry on molecular mobility and morphology of multiwalled carbon nanotubes epoxy nanocomposite. Polymer, 48, 5662-5670.

14. Chowdhury, F.H., Hosur, M.V., and Jeelani, S. (2006) Studies on the flexural and thermomechanical properties of woven carbon/nanoclay-epoxy laminates. Materials Science & Engineering, A, 421, 298-306.

15. Wouterson, E.M., Boey, F.Y.C., Hu, X., and Wong, S.C. (2007) Effect of fiber reinforcement on the tensile, fracture and thermal properties of syntactic foam. Polymer, 48, 3183-3191.

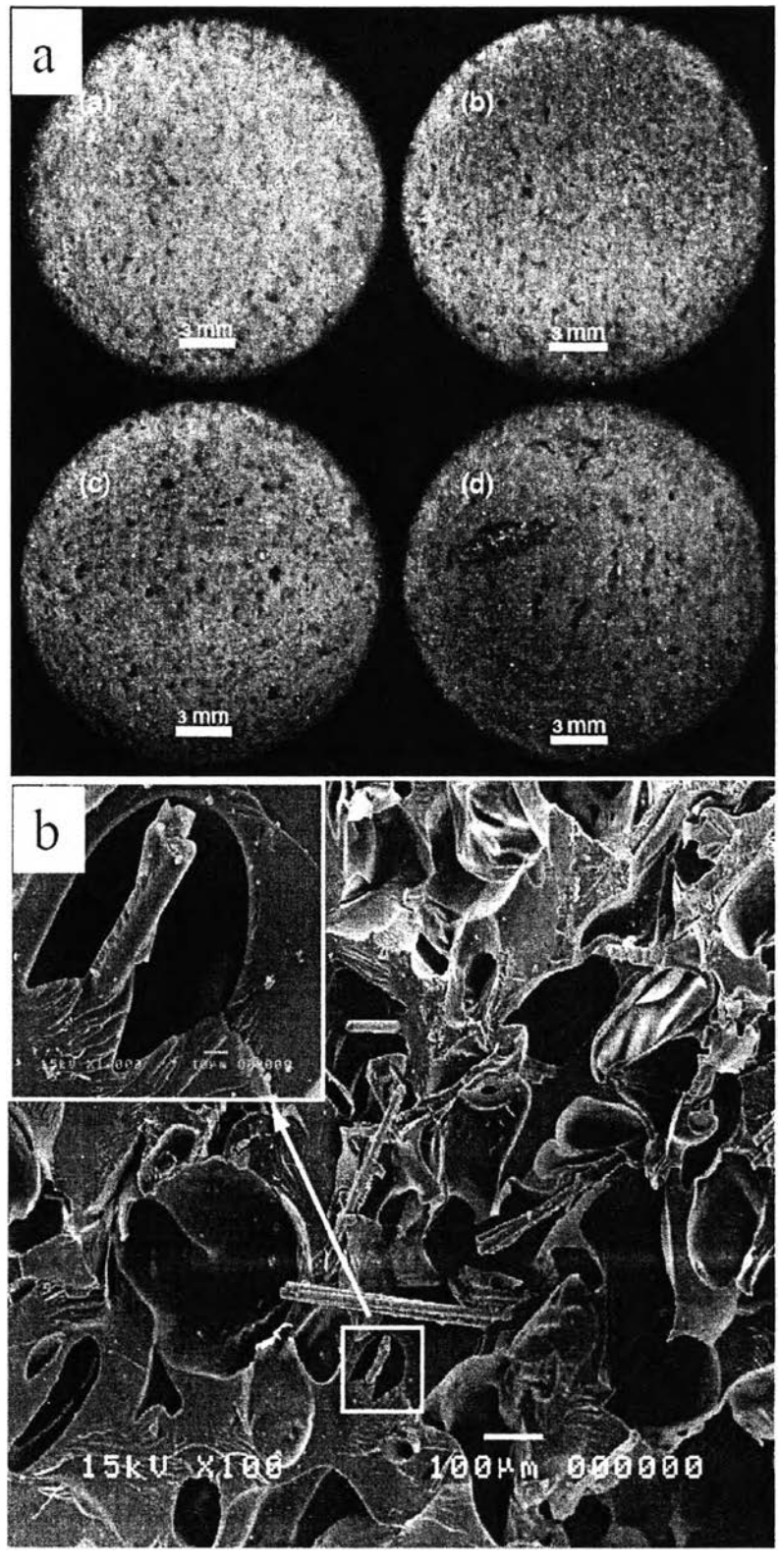

Figure 7.1 Microscope images of polybenzoxazine foam composites with different fiber contents (a) SEM micrograph of 3 wt% of fiber reinforced foam composite (b).

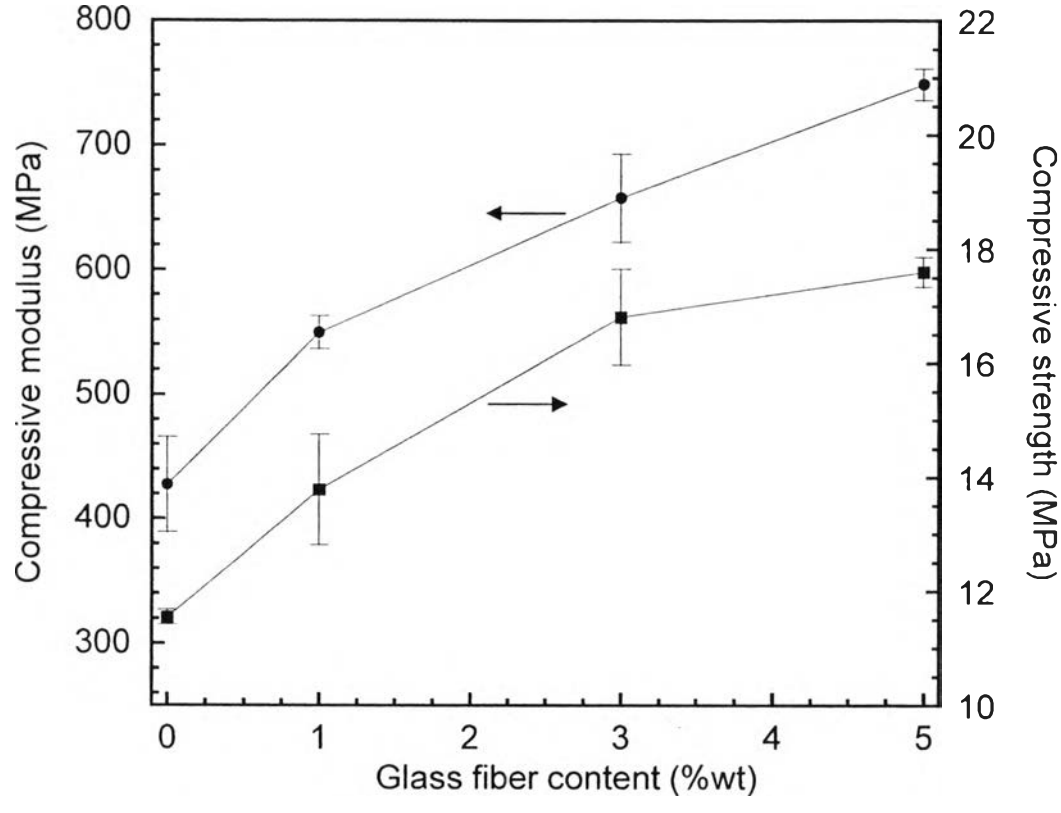

Figure 7.2 Compressive strength and modulus of polybenzoxazine foam composites as a function of fiber content.

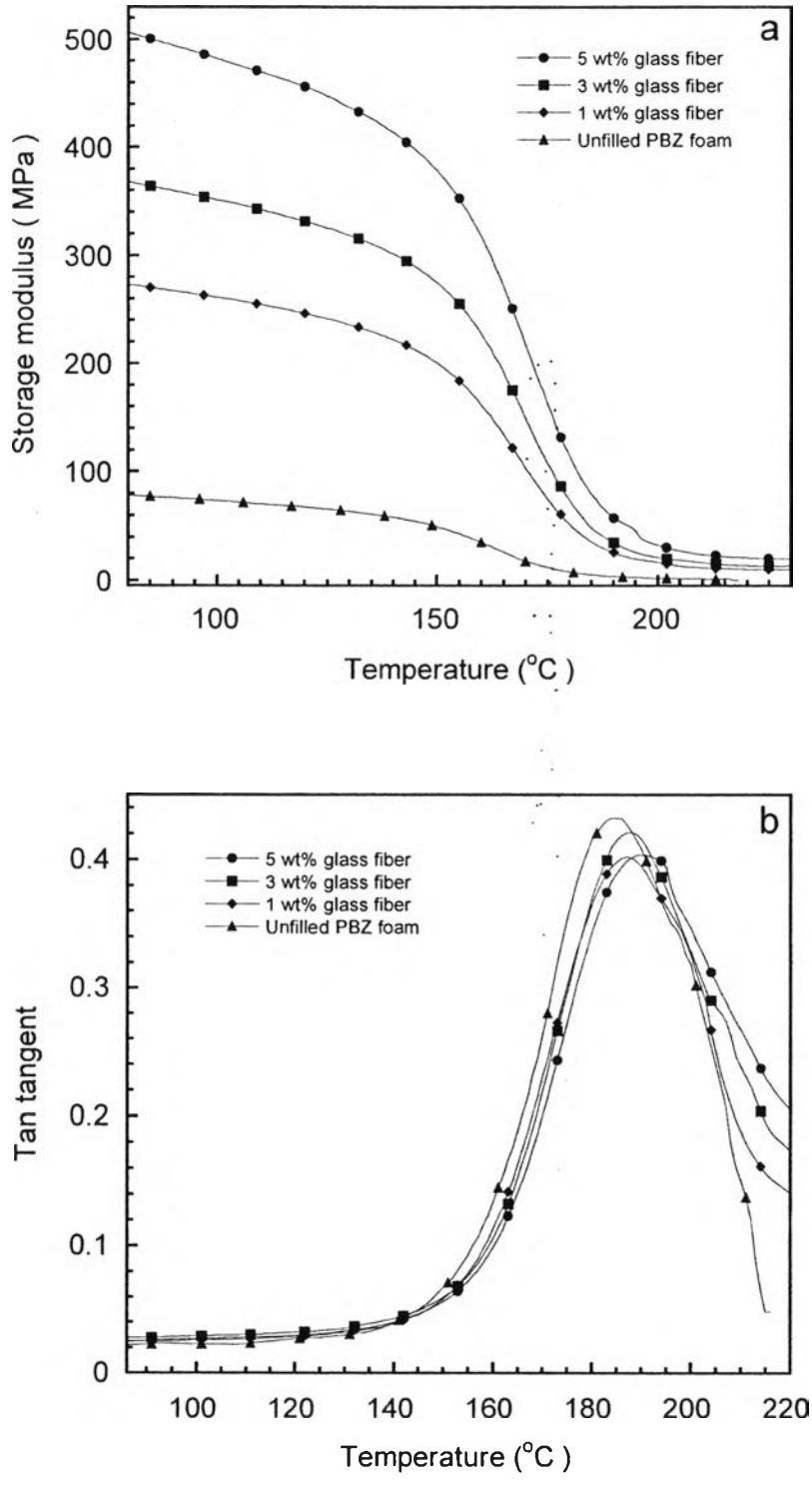

Figure 7.3 Storage modulus (a) loss tangent (b) of polybenzoxazine foam composites with different fiber contents.

Table 7.1 Physical, compressive, and thermal properties of polybenzoxazine foam composites with different fiber contents

Glass fiber Content (wt%)	Specific compressive strength ($MPa/g/cm^3$)	Specific compressive modulus ($MPa/g/cm^3$)	Compressive strength increment (%)	Compressive modulus increment (%)	Glass transition temperature (°C)
0%	32.1 ± 0.5	1185.9 ± 88.1	0.0	0.0	184
1%	35.4 ± 2.5	1413.8 ± 46.4	19.4	28.6	187
3%	38.7 ± 1.9	1513.5 ± 75.6	45.6	53.8	188
5%	38.3 ± 0.6	1629.6 ± 31.5	52.5	75.2	190